Biomedicine & Pharmacotherapy 123 (2020) 109794

Contents lists available at ScienceDirect

Biomedicine & Pharmacotherapy

journal homepage: www.elsevier.com/locate/biopha

Berberine associated photodynamic therapy promotes autophagy and apoptosis via ROS generation in renal carcinoma cells

Tairine Zara Lopes[a], Fabio Rogério de Moraes[b,c], Antonio Claudio Tedesco[d], Raghuvir Krishnaswamy Arni[b,c], Paula Rahal[a], Marilia Freitas Calmon[a,*]

[a] Laboratory of Genomics Studies, São Paulo State University, São José do Rio Preto, São Paulo, Brazil
[b] Physics Department, São Paulo State University, São José do Rio Preto, São Paulo, Brazil
[c] Multiuser Center for Biomolecular Innovation, São Paulo State University, São José do Rio Preto, São Paulo, Brazil
[d] Department of Chemistry, Center of Nanotechnology and Tissue Engineering-Photobiology and Photomedicine Research Group, Faculty of Philosophy, Sciences and Letters of Ribeirao Preto, University of São Paulo, Ribeirao Preto, SP, Brazil

ARTICLE INFO

Keywords:
Berberine
Cell death
Photodynamic therapy
Renal cell carcinoma

ABSTRACT

Renal cell carcinoma (RCC) consists of the most lethal common urological cancer and the clinical practice has shown that resistant RCC to commons therapies is extremely high. Berberine is an isoquinoline alkaloid, presents in different kinds of plants and it has long been used in Chinese medicine. It has several properties, such as antioxidant, anti-inflammatory, anti-diabetic, anti-microbial and anti-cancer. Moreover, berberine has photosensitive characteristics and its association with photodynamic therapy (PDT) is effective against tumor cells. This study aimed to evaluate the effects of berberine associated with PDT in renal carcinoma cell lines. The cellular viability assay showed increased cytotoxicity in concentration and time-dependent manner. Berberine presented efficient internalization in all cell lines analyzed. In addition, after treatment with berberine associated with PDT, it was observed a high phototoxicity effect with less than 20 % of viable cells. In this study we observed that the increase of reactive oxygen species (ROS) levels was accompanied by an increase of autophagy levels and apoptosis by caspase 3 activity, suggesting cell death by both mechanisms. Additionally, three target genes of anti-cancer drugs were differentially expressed in 786-O cells, being that Vascular Endothelial Growth Factor-D (*FIGF*) and Human Telomerase Reverse Transcriptase (*TERT*) gene presented low expression and Polo Like Kinase 3 (*PLK3*) presented overexpression after treatment with berberine associated with PDT. In this study, the proposed treatment triggered metabolites changes related to cell proliferation, tumorigenesis and angiogenesis. Thus, it was possible to suggest that berberine has promising potential as a photosensitizing agent in a photodynamic therapy, because it induced significant anticancer effects on renal carcinoma cells.

1. Introduction

Renal cell carcinoma (RCC) is the 9th most common cancer in men and 14th most common in women worldwide and consists in the most lethal common urological cancer, with mortality of 30–40 % [1,2]. RCC accounts for 2–3% of all cancers and worldwide more than 338,000 new cases are diagnosed each year [3]. Usually, the surgery is the mainstay for curative treatment for RCC, followed by adjuvant therapies such as radiotherapy and chemotherapy. Clinical practice has shown that the percentage of resistant RCC to commons therapies is extremely high [1,4]. Despite the surgery is the main treatment, more than 40 % of patients develop metastatic disease after nephrectomy with poor prognosis and low survival rate [5]. Additionally, the side effects are several, including hematological toxicity, gastrointestinal disorders, cardiovascular alterations, chemoresistance, and moreover emotional debilitation [6,7]. Thus, there is a high demand for other locally targeted therapeutics strategies and new protocols that increase treatment efficacy, to improve patient life quality and survival. In this context, the use of phytochemicals extracted from various vegetables, fruits, herbs, and medicinal plants has attracted great attention and has been extensively investigated for anticancer properties [8].

Berberine (BBR) is an isoquinoline alkaloid presents in roots, rhizome, and stem bark of many kinds of plants and it has long been used in Chinese medicine [9]. It has antioxidant, anti-inflammatory, anti-diabetic, anti-microbial and anti-cancer properties [10]. Previous studies showed that berberine directly binds to DNA in a pH-dependent

* Corresponding author at: Department of Biology, Instituto de Biociências, Letras e Ciências Exatas – IBILCE/UNESP, Cristóvão Colombo, 2265, 15054-000 São José do Rio Preto, SP, Brazil.
E-mail address: marilia.calmon@unesp.br (M.F. Calmon).

https://doi.org/10.1016/j.biopha.2019.109794
Received 3 September 2019; Received in revised form 5 December 2019; Accepted 10 December 2019

manner, establishing a DNA-berberine complex [11]. Moreover, several mechanisms have been involved in the antitumor activity of berberine, including induction of cell cycle arrest, inhibition of cell proliferation and migration and stimulation of apoptosis in various cancer cell lines [12–15], but the molecular mechanisms are not completely elucidated for each type of cancer [16].

The fluorescent nature of berberine is a good indicator for the photodynamic process [17], thus it might be used as a new type of photodynamic therapeutic agent [18]. Some authors have reported that berberine is a photosensitive agent with the ability to generate reactive oxygen species and other radicals in the presence of light source [19,20]. Therefore, berberine can be considered as a photosensitizer candidate in Photodynamic Therapy (PDT), potentializing treatment efficiency and minimizing the side effects.

In this context, photodynamic therapy (PDT) is a noninvasive treatment method with a local target that has been presented as a potential approach for oncological diseases [21,22]. PDT involves threes essential components – photosensitizing agent, a visible light source and molecular oxygen. These components together are able to initiate a photochemical reaction that results in the generation of reactive oxygen species (ROS) (e.g., singlet oxygen, superoxide anion radical, hydrogen peroxide, etc.), which are highly cytotoxic [23,24]. The production of ROS at mitochondrial, lysosomal or endoplasmic reticulum loci can lead to an irreversible damage of tumor cells and initiate cell death by several mechanisms [25]. Both autophagy and apoptosis have previously been reported to be the response of oxidative stress and energy privation [26]. After a stress stimulus, ROS can lead to the formation of autophagosome, and previous studies demonstrated that ROS play an important role in promoting autophagy [27].

Generally, apoptosis is the main type of cell death in PDT occurring quite rapidly after photodamage, characterized by fragmentation of DNA and condensation of chromatin [28]. The localization of photosensitizer (PS) is essential to determine the type of cell death and apoptosis can occur when PS is located mitochondrially [29].

Therefore, this present research evaluated the effect of berberine associated PDT in renal carcinoma cell lines.

2. Material and methods

2.1. Preparation of the berberine

Berberine chloride was purchased from Sigma Aldrich (St Louis, MO, USA). Berberine was dissolved in Dimethyl sulfoxide – DMSO (Sigma Aldrich, St Louis, MO, USA) to perform all of the experiments of this study.

2.2. Cell lines and culture conditions

Human RCC cell lines (ACHN, 786-O) and human renal tubular epithelial cells derived from normal kidneys (HK-2) were obtained from American Type Culture Collection (ATCC, Manassas, VA, USA). ACHN cells were cultured in a Mem Alpha Medium (Gibco by Life Technologies, Grand Island, NY, USA), 786-O cells were cultured in RPMI1640 medium (Gibco by Life Technologies, Grand Island, NY, USA) and HK-2 cells were cultured in keratinocyte serum-free medium (K-SFM) (Gibco by Life Technologies, Grand Island, NY, USA). The Mem Alpha and RPMI1640 medium were supplemented with 10 % fetal bovine serum (FBS; Cultlab, Campinas, Sao Paulo, Brazil), 100 U/mL penicillin (Gibco, Life Technologies, Carlsbad, California, USA), and 100 mg/mL streptomycin (Gibco, Life Technologies, Carlsbad, California, USA) and K-SFM were supplemented with 5 % fetal bovine serum (FBS; Cultlab, Campinas, Sao Paulo, Brazil), 25 mg bovine pituitary extract and 2,5 µg recombinant epithelial growth factor per ml. All cells were cultured at 37 °C in a humid atmosphere with 5 % CO_2.

2.3. Cell viability assay

The cell lines were seeded at the density of $1,5 \times 10^4$ cells/well in 96-well plates for 24 h. The cells were treated with several concentrations of BBR (5µM, 10 µM, 20 µM, 40 µM, 80 µM, 160 µM, and 320 µM). After 24 and 48 h of treatment, 1 mg/mL of 3-(4,5-dimethylthiazol-2-yl)-2,5-diphenyl-tetrazolium bromide (MTT) (Sigma Aldrich, St Louis, MO, USA) was diluted to 100 µL of the medium in each well and incubated for 30 min at 37 °C. Then, the MTT was removed and 100 µL of DMSO (Sigma-Aldrich, St. Louis, Missouri, USA) added to solubilize the formazan crystals and the absorbance was read using a microplate reader (Fluostar Omega, BMG Labtech, *Ortenberg*, Germany) at a wavelength of 570 nm. All experiments were performed in triplicate and in three independent assays.

2.4. Cellular uptake of the BBR

To analyze the intracellular uptake of BBR 3×10^5 cells/well were seeded in 6-well plates. The ACHN, 786-O, and HK-2 cells were treated with 20 µM of BBR. After 3, 6, 12, 24 and 48 h of incubation the cells were washed with PBS, then viewed and photographed using a fluorescence microscope (Zeiss Axio Vert. A1) with a FITC filter (excitation spectra: 489 nm, blue laser, 415 ± 15 nm, FITC). The fluorescence of the BBR is detected by excitation at 421 nm and emission at 555 nm [30].

2.5. Cell viability and phototoxicity

ACHN, 786-O, and HK-2 were seeded at the density of $1,5 \times 10^4$ cells/well in 96-well plates for 24 h and they were incubated for 3 h with BBR (20 µM). After the incubation time, the cells were washed with PBS and 100 µL of fresh culture medium without phenol red and FBS was added to each well. To irradiation it was used a laser (Vet Light – DMC Enterprise, Sao Carlos, Sao Paulo, Brazil), operating at 447 nm and 80 J/cm^2 of fluency, set at 4 min for application. After irradiation, 100 µL of fresh culture medium with 10 % FBS was added to each well. Then, cell viability was measured after 24 h of irradiation by MTT assay. In this experiment four types of treatment were established: cells without treatment (control), cells treated with BBR but not exposed to laser; cells exposed to laser only and cells treated with BBR and exposed to the laser. All experiments were performed in triplicate and in three independent assays.

2.6. Measurement of reactive oxygen species (ROS) assay

The intracellular ROS generation was measured using a 2′-7′-dichlorofluorescin diacetate (DCFDA) – *Cellular Reactive Oxygen Species Detection Assay Kit* (ab113851, Abcam, Cambridge, UK) with slight modifications. DCFDA is a fluorogenic dye that measures hydroxyl, peroxyl and other ROS activity within the cell. In the presence of ROS, this compound is oxidized within the cell and produces a fluorescent compound, 2′, 7′-dichlorofluorescein (DCF), which remains intracellular. Briefly, ACHN, 786-O, and HK-2 cell lines were seeded in 96-well plates. On the following day, cells were incubated with BBR (20 µM) associated PDT. After 24 h of treatment, cells were incubated with culture medium containing 25 µM DCFDA for 45 min at 37 °C. Then, the ROS level was determined by measuring the fluorescence intensity using a microplate reader (Fluostar Omega, BMG Labtech, *Ortenberg*, Germany) with excitation and emission wavelengths set at 485 and 535 nm, respectively. Tert-butyl hydrogen peroxide (TBHP), which induces ROS activity to reduce DCFDA to DCF, was used as the positive control. All experiments were performed in triplicate and in three independent assays.

2.7. Autophagy assay

Autophagy was analyzed using an *Autophagy Assay Kit* (MAK138, Sigma-Aldrich, St. Louis, MO, USA) according to the manufacturer's protocol. Briefly, ACHN, 786-O, and HK-2 cell lines were seeded in 96-

well plates and treated with BBR associated PDT. After 24 h of treatment, cells were incubated with Autophagosome Detection Reagent diluted in Stain buffer for 1 h at 37 °C. Next, wells were washed with wash buffer and following it was performed a reading of fluorescence intensity of intracellular autophagosomes with excitation and emission wavelengths set at 360 and 520 nm, respectively. Trichostatin A (TSA), which induces autophagy process, was used as the positive control. All experiments were performed in triplicate and in three independent assays.

2.8. Apoptosis assay

The caspase 3 activities in ACHN, 786-O, and HK-2 cells were measured using a *Caspase 3 Assay Kit Colorimetric* (ab39401, Abcam, Cambridge, UK) with slight modifications. Briefly, 3×10^5 cells in 6-well plates were seeded and treated with BBR associated PDT. After 24 h of treatment, cells were resuspended in 50 µl of Cell Lysis Buffer, cell supernatant was isolated and measurement of protein concentration was performed by ND-2000 Nanodrop (Thermo Scientific, Wilmington, DE, USA). Then, 25 µl of 2× Reaction Buffer (containing 10 mM DTT) and 2,5 µl of 4 mM DEVD-p-NA substrate were added into 25 µl of each sample and the cells were incubated for 2 h at 37 °C. The absorbance was detected at the wavelength of 405 nm. The caspase 3 activity was determined to compare treated cells results with the untreated control. All experiments were performed in triplicate and in three independent assays.

2.9. PCR array

Total RNA from 786-O cells after 1 h of treatment with BBR associated PDT and 786-O cells without treatment were isolated using the RNeasy mini kit according to the manufacturer's instructions (Qiagen, Germany). Total RNA (2 µg) from each group of 786-O cells was reverse transcribed using the first-strand cDNA synthesis kit for RT-PCR (Qiagen, Germany), following the manufacturer's instructions. Nuclease-free water was used to dilute the amplified cDNA and was added to the RT^{2}qPCR SYBR green Master Mix (Qiagen, Germany). After, 25 µl of the experimental cocktail was added to each well of the *Human Cancer Drug Targets RT^2 Profiler PCR array* (Qiagen, Germany). Real-time PCR was performed on the Applied Biosystems 7300 Real-Time PCR System (Applied Biosystems, USA) according to the manufacturer's instructions (Qiagen, Germany). All data from the PCR was collected and differential expression of genes was analyzed by Qiagen Web Portal (https://www.qiagen.com/br/shop/genes-and-pathways/data-analysis-center-overview-page/).

2.10. Metabolite footprinting analysis

Intracellular and extracellular metabolite levels are correlated as intake and secretion are controlled events by several cytosolic and transmembrane proteins [31,32]. Therefore, the culture medium from 786-O control cells and 786-O cells after treatment with berberine associated with PDT were used to assess metabolic changes. Briefly, 1×10^6 cells were seeded in dishes (60 mm) and treated with BBR associated PDT. After 30 min, 3 h and 6 h of treatment, the culture media were collected for analyses of extracellular metabolites. As external reference, DSS was added to 500 µM in order to measure relative concentrations.

2.11. Nuclear magnetic resonance spectroscopy

Cell medium was transferred to NMR 5 mm tubes and added 10 % D_2O for tune and match procedures. Data were collected at 298 K in a 600 MHz Bruker AVANCE III HD magnet. All ^{1}H NMR measurements were performed by a pre-saturated Call-Purcell-Meiboom-Gill (CPMG) pulse sequence. A 14 ppm (parts per million) slide window was chosen, with a relaxation delay of 5 s. Spin-echo delay was set to 400 µs with 400 loop T_2 filter. A total of 64 scans were acquired. Free induction decays (FIDs) were multiplied by an exponential function with a 1 Hz line broadening prior to Fourier transformation. Topspin 3.5 (Bruker Biospin, Germany) was used to manually phase and baseline correction. Total correlation spectroscopy (TOCSY) and heteronuclear single quantum coherence (HSQC) spectroscopy were performed using Bruker standard pulse sequences for selected samples, in order to assist metabolite assignment.

2.12. Statistical analysis

Data were expressed as mean ± standard deviation. Statistical analyses were performed using GraphPad Prism 7 Software (GraphPad Software Inc., San Diego, CA, USA) and the statistical significance of differences between the results was determined by analysis of variance (ANOVA) followed by post-test Tukey's test for multiple comparisons. $p \leq 0.05$ was considered statistically significant in this study.

NMR data was assigned to different metabolites using Chenomx software (Chenomxs Inc. Alberta, Canada) and the Human Metabolome Database [33]. After metabolite assignment, MetaboAnalyst 4.0 [34] was used with the relative concentrations of each metabolite, as referred to DSS concentration. The same scaling and normalization was repeated. Statistical analysis was performed by using PCA, Partial Least Square Discriminant Analysis (PLS-DA) and its orthogonal version (OPLS-DA), and subjected to Welch *t*-test as available in MetaboAnalyst.

Evaluation of the selected metabolites for discriminating metabolic changes in cell culture was carried out by a Support Vector Machine (SVM) classification algorithm accessible at the Biomarker Analysis module in MetaboAnalyst. SVM uses combinations of metabolite levels, selected by built-in feature ranking, and by leave-one-out cross validation (used to repeat multiple times SVM training and evaluation). If there are differences in the measured levels between populations, it is expected the method to have high area under the curve (AUC) in Receiver Operating Characteristic (ROC) curves. The frequency of appearance of each metabolite to compose the classification in SVM is indication of the relevance for the metabolites.

3. Results

3.1. Effects of the BBR on cell viability

To investigate the effects of BBR on ACHN, 786-O, and HK-2 cell lines, we first evaluated the cytotoxicity of BBR in different concentrations (5, 10, 20, 40, 80, 160 and 320 µM) after 24 and 48 h of incubation by MTT assay.

The cell viability was affected by BBR in a dose-dependent manner (Fig. 1). All the cell lines presented high cellular viability (> 80 %) in the concentration until 40 µM in 24 h, however, the HK-2 cells treated with 40 µM of BBR presented viability < 80 % in 48 h. For this reason, it was chosen the concentration of 20 µM to perform the next experiments. In general, BBR showed low cytotoxicity in the dark in the cell lines being considered a good photosensitizer for photodynamic therapy.

3.2. Cellular uptake of BBR

Fluorescence microscopy was used to evaluate the cellular uptake of BBR after 3, 6, 12, 24 and 48 h of incubation. The cells ACHN, 786-O, and HK-2 were able to internalize 20 µM of BBR after 3 h of BBR incubation. On the other side, the fluorescence decreases for all cell lines after 24 and 48 h of BBR incubation (Fig. 2). The results showed that BBR is dispersed by the cytosol and nucleus in all the cell lines evaluated.

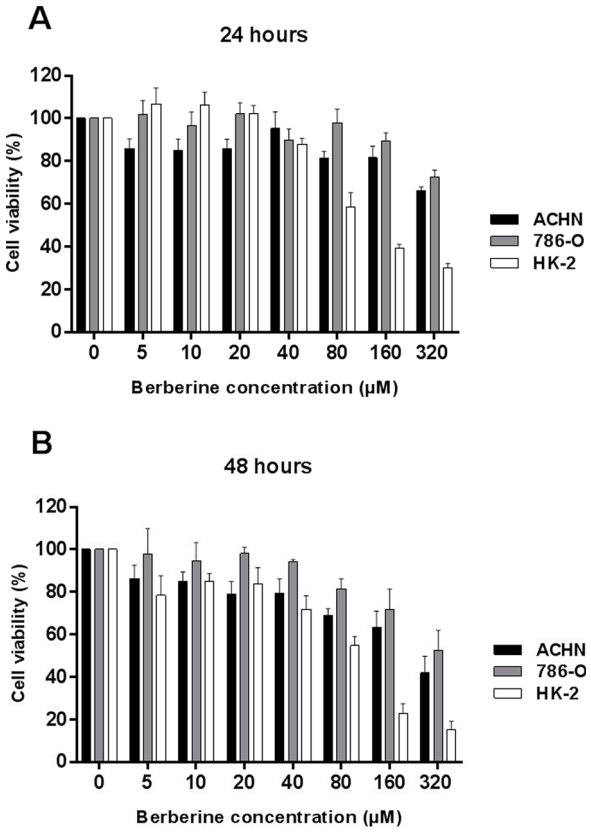

Fig. 1. Cytotoxicity of berberine on ACHN, 786-O and HK-2 cells. The ACHN, 786-O and HK-2 cells were treated with different concentrations (5 μM, 10 μM, 20 μM, 40 μM, 80 μM, 160 μM and 320μM). (A) Cellular viability of the cell lines 24 h after BBR incubation. (B) Cellular viability of the cell lines 48 h after BBR incubation. All assays were performed in triplicate, and data shown are mean ± SD of three independent experiments.

3.3. Effects of the phototoxicity of the BBR

Cell lines treated with BBR presented high cellular viability being 91.6 % for ACHN, 78.9 % for 786-O and 88.8 % for HK-2 cells. The cell lines treated only with the laser without BBR also showed high cellular viability: ACHN cell presented 90.64 % of viability, 87.80 % for 786-O cells and 93 % for HK-2 cells. On the other hand, ACHN, 786-O, and HK-2 treated with BBR associated with PDT showed a significant decrease in the cellular viability compared to the control cells: 16.26 % of cellular viability in ACHN cells ($p < 0.0001$), 16.33 % in 786-O cells ($p < 0.0001$) and 15.89 % in HK-2 cells ($p < 0.001$) (Fig. 3). These results demonstrated the promising phototoxic effect of BBR associated with PDT for all renal carcinoma cell lines evaluated. It was observed that HK-2 cells showed greater sensibility in relation to ACHN and 786-O cells but the treatment with PDT is locally targeted decreasing the effects over non-tumoral cells.

3.4. BBR associated with PDT induces ROS generation

Accumulation of ROS in ACHN, 786-O, and HK-2 cells was analyzed by DCFDA staining. Levels of ROS in the cell treated only with BBR and laser alone were similar to control. In contrast, cells treated with BBR associated with PDT showed a significant increase in the ROS generation, being that ACHN, 786-O, and HK-2 cells presented an increase of 180.03 % ($p < 0.0001$), 152.65 % ($p < 0.0001$), 156.65 % ($p < 0.0001$) respectively (Fig. 4).

3.5. BBR associated with PDT induces autophagy

Autophagosome detection was analyzed by fluorescence intensity. It was shown that BBR associated with PDT induced autophagic processes in all cell lines analyzed. All cell lines treated with BBR alone showed levels of autophagy slightly more than 115 % and laser alone showed levels similar to control. On the other hand, cells treated with BBR associated PDT presented a significant increase in the levels of autophagy. The cells ACHN, 786-O, and HK-2 presented 173.2 % ($p < 0.0001$), 175 % ($p < 0.0001$) and 169 % ($p < 0.0001$) of autophagy respectively (Fig. 5).

These results suggest that BBR photoactivation leads to autophagosome formation and consequently, cell death by autophagy.

3.6. BBR associated with PDT induces apoptosis

Caspase 3 activity in ACHN, 786-O, and HK-2 cells were measured using a *Caspase 3 Assay Kit Colorimetric* after BBR and PDT treatment. The caspase 3 activity similar to the control group were observed in the cells of the groups treated only with BBR and only with laser. In contrast, we observed that renal carcinoma cells treated with BBR associated with PDT showed a significant increase of caspase 3 activity (141.8 % in ACHN cells, $p < 0.01$) and 190.64 % in 786-O cells, $p < 0.0001$). The caspase-3 activity in non-tumoral cells (HK-2) treated with berberine associated with PDT was slight significant ($p = 0.05$) with a percentage of 120.64 % in comparison to the control group (Fig. 6). These results showed that BBR associated PDT is able to activate caspase 3 leading cell death by apoptosis in renal carcinoma cells.

3.7. Expression of Target Genes of Anti-Cancer Drugs in 786-O cells treated with BBR associated with PDT

To evaluate possible target genes of anti-cancer drugs and its gene expression profile of the 786-O cells without treatment and BBR associated with PDT was used RT^2 Profiler PCR arrays. Target genes of anti-cancer drugs with differential expression between 786-O cells are represented in Table 1. We can observe that *FIGF* ($p = 0.02$) and *TERT* ($p = 0.05$) genes presented reduced expression, while the *PLK3* was upregulated ($p < 0.001$) after BBR associated with PDT treatment.

3.8. Metabolic changes induced by BBR associated with PDT

Nuclear magnetic resonance spectroscopy successfully identified several signals from the metabolite in 786-O (Table 2) cell line. As shown in Fig. 7 and respective table, up to 24 different metabolites were identified and quantified in NMR spectra for each time period. Relative concentrations are shown as box plots for each individual metabolite after 30 min, 3 h and 6 h post treatment (Figures S1–S8).

PCA score plots indicate that metabolic changes are not notable for up to 3 h post treatment for 786-O (Figure S9). Nevertheless, after 6 h post treatment, cells seem to have metabolic changes that were measured by the NMR-based metabolomics approach used. In addition, PCA is not a supervised approach and, as such, distances between control and treated samples are not optimized. On the other hand, PLS-DA and OPLS-DA are better in discriminating control and treated groups, as they use this information to maximize the distances between groups. OPLS-DA score plot were able to distinguish the metabolic signature between control and treated samples after only 30 min following treatment (Figure S9). In order to check which metabolites and, thus, their corresponding metabolic pathway were mainly affected by treatment with berberine associated with PDT, a support vector machine (SVM) classification system was set, using MetaboAnalyst. By using metabolites levels from 70 % of the samples in each time period, a SVM was trained and the model was evaluated using 30 % of the remaining samples. This was repeated multiple times, so, every sample was used for both training and evaluation in different steps. As it could be

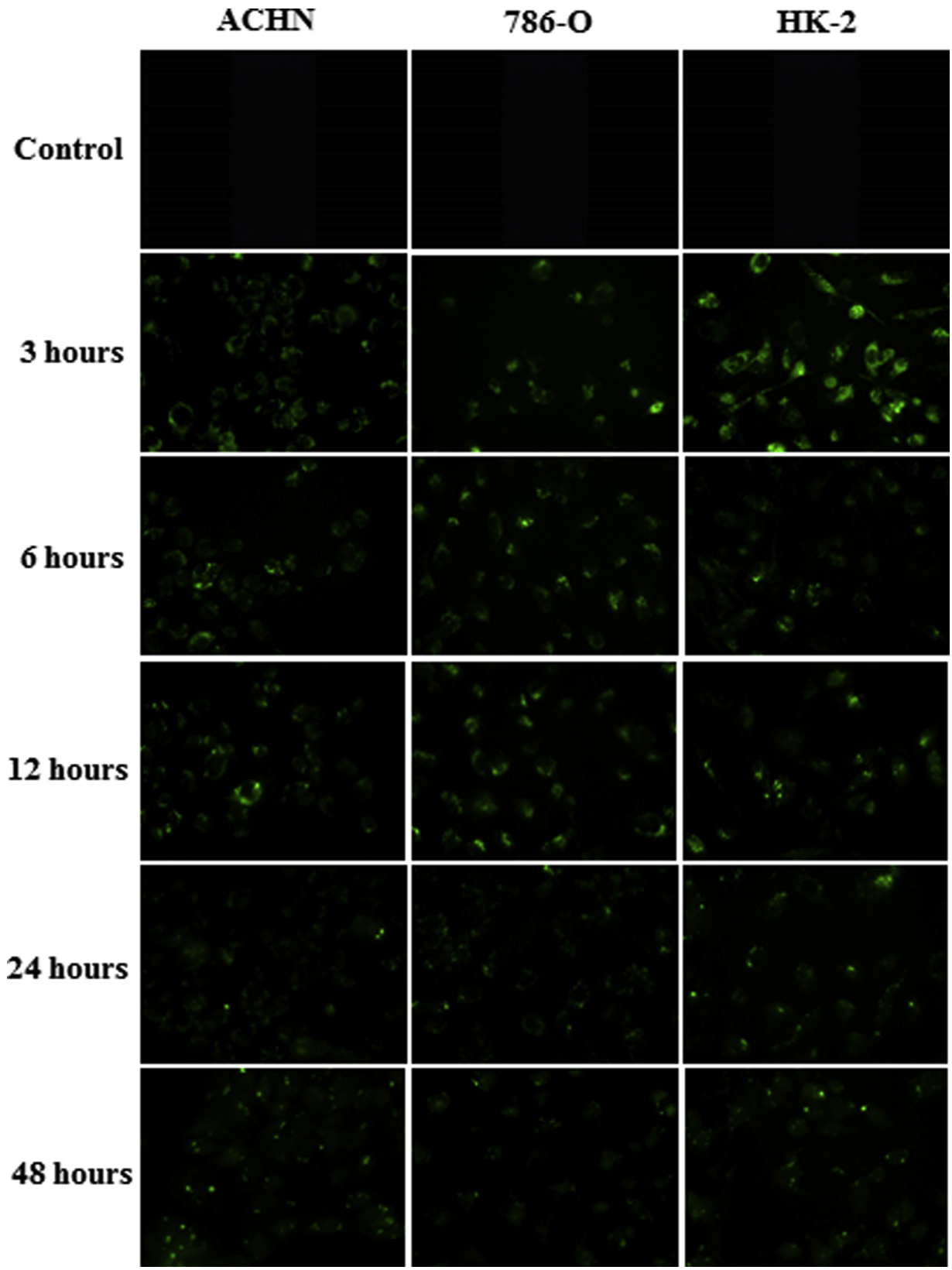

Fig. 2. Fluorescence microscopy images of cellular uptake of BBR (20 μM) after different periods of BBR incubation. The pictures were taken 3, 6, 12, 24 and 48 h after BBR incubation. Scale bar: 20 μm.

expected from OPLS-DA score plots, it was found that SVM has good accuracy in discriminant metabolite levels between control and berberine associated with PDT treated samples. MetaboAnalyst SVM approach uses a subset of metabolites for each run and, consequently, the frequency of usage for each metabolite in top scoring models are an indicative of most affected metabolites (and pathways), as they would have more different concentrations between control and treated samples.

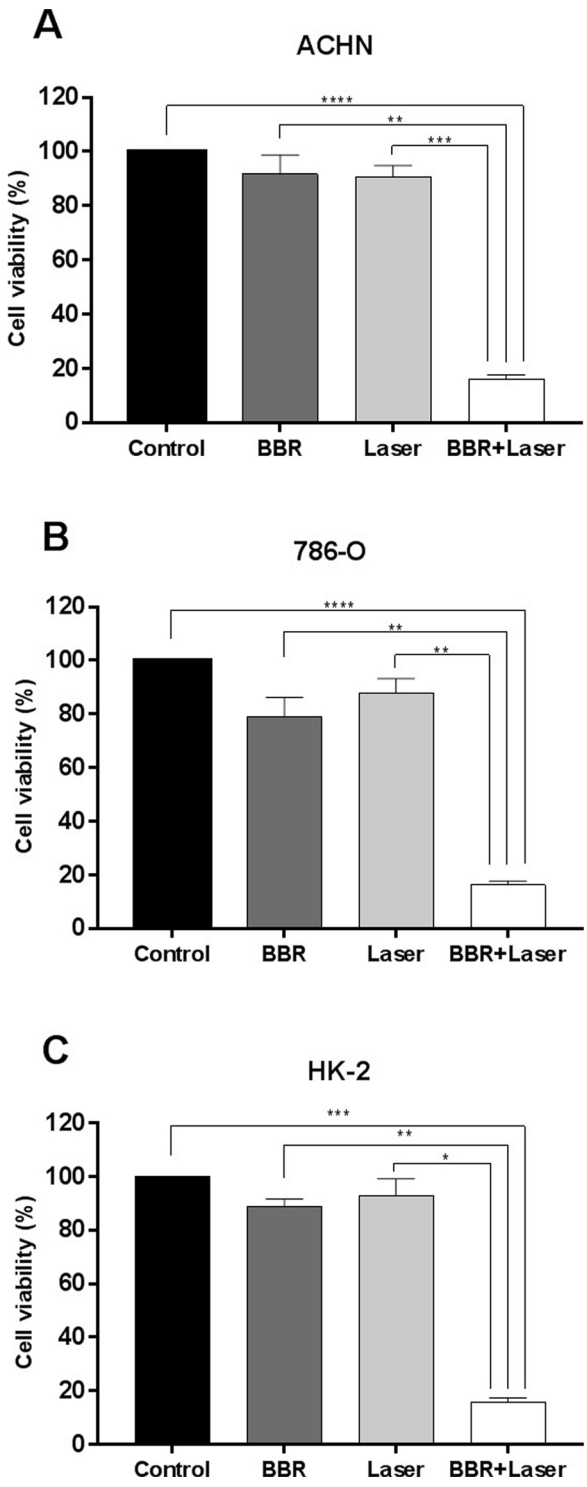

Fig. 3. Phototoxicity assay in ACHN (A), 786-O (B) and HK-2 (C) cells. The cellular viability was evaluated 24 h after laser irradiation. All assays were performed in triplicate, and data shown are mean ± SD of three independent experiments. * $p < 0.05$; ** $p < 0.01$; *** $p < 0.001$; **** $p < 0.0001$. Control = without any treatment; BBR = berberine only; Laser = laser only; BBR + Laser = berberine associated with photodynamic therapy.

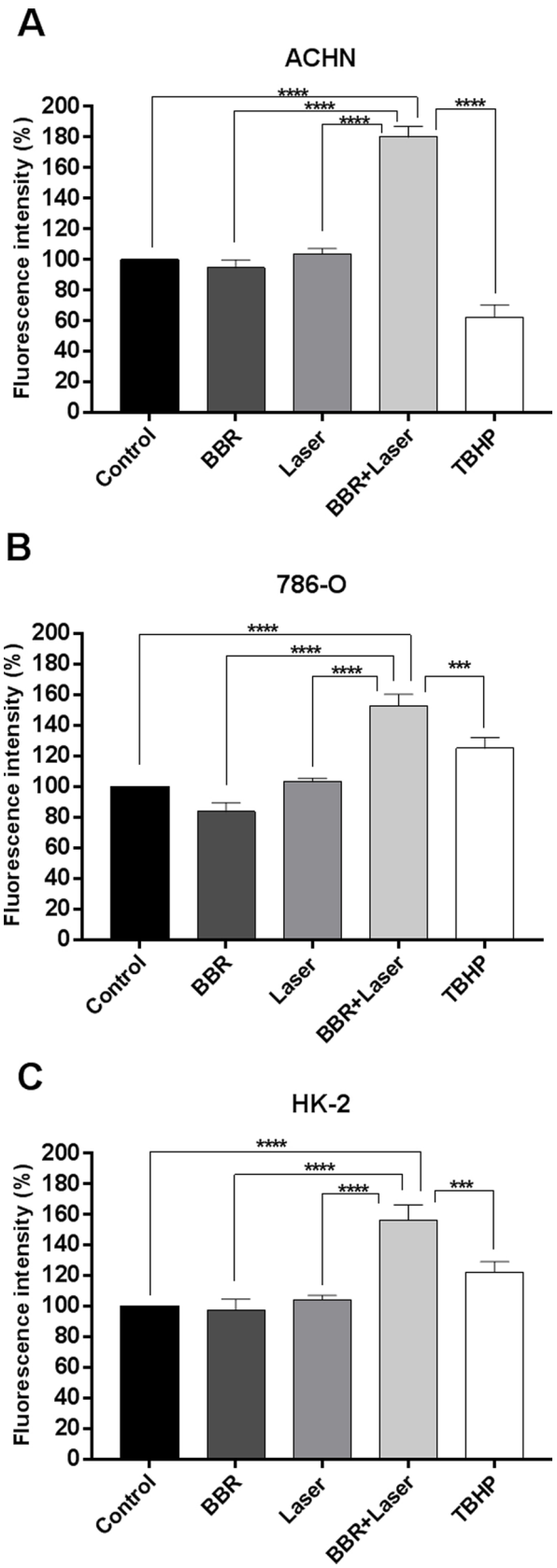

Fig. 4. ROS generation in ACHN (A), 786-O (B) and HK-2 (C) cell lines. All assays were performed in triplicate, and data shown are mean ± SD of three independent experiments. *** $p < 0.001$; **** $p < 0.0001$. Control = without any treatment; BBR = berberine only; Laser = laser only; BBR + Laser = berberine associated with photodynamic therapy; TBHP = hydrogen peroxide (positive control).

In this study, several metabolites statistically significant were detected in 786-O cells after treatment with BBR associated PDT and are represented in Table 2.

We can highlight some metabolites with statistical significance that may be related to the processes of cell proliferation and tumorigenesis. Metabolite analyzes showed that the level lysine had a significant

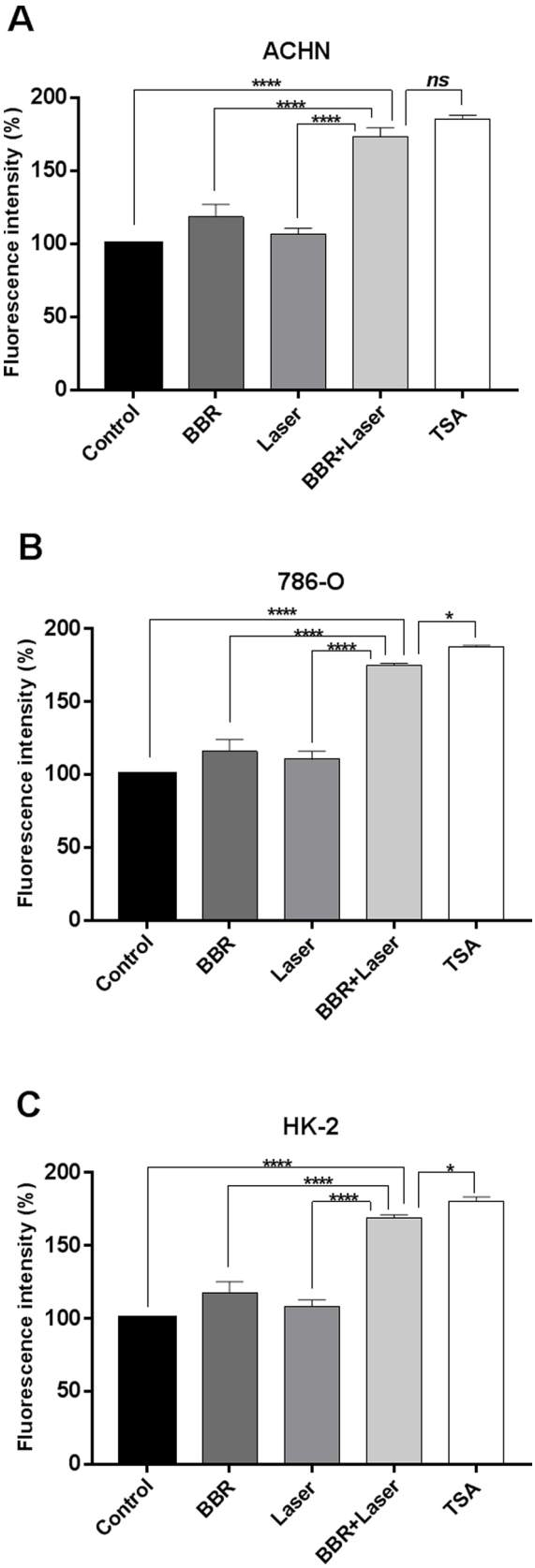

Fig. 5. Autophagy in ACHN (A), 786-O (B) and HK-2 (C) cell lines. All assays were performed in triplicate, and data shown are mean ± SD of three independent experiments. * $p < 0.05$; **** $p < 0.0001$, *ns:* no significant. Control = without any treatment; BBR = berberine only; Laser = laser only; BBR + Laser = berberine associated with photodynamic therapy; TSA = trichostatin A (positive control).

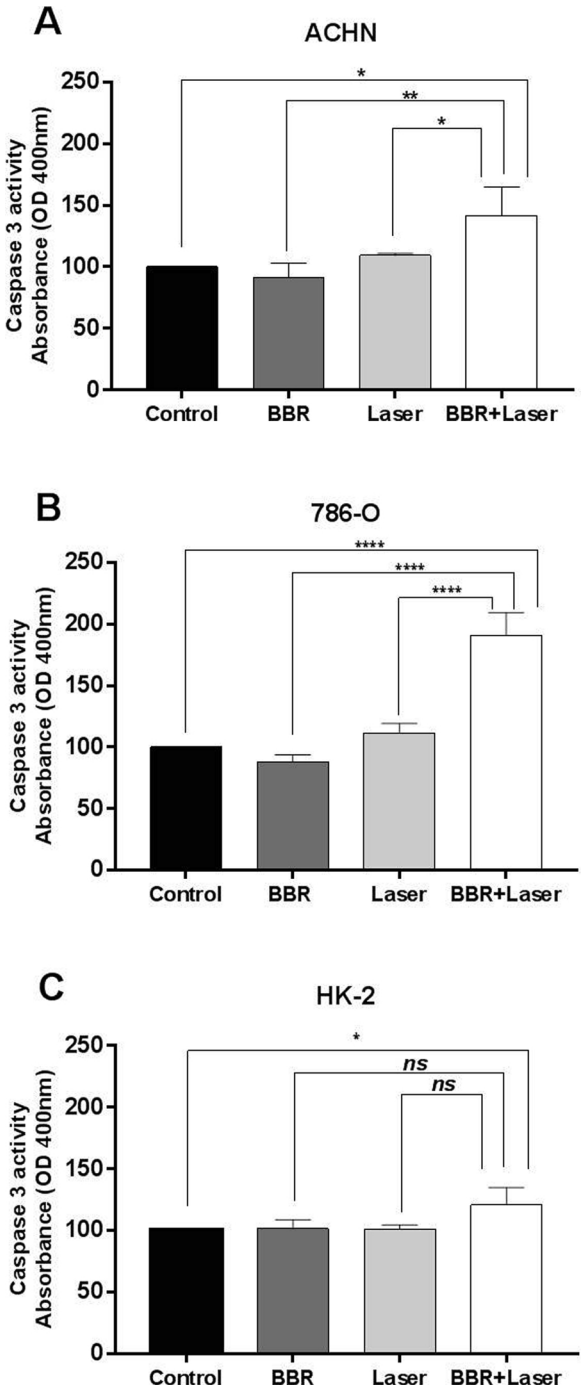

Fig. 6. Caspase 3 activity in ACHN (A), 786-O (B) and HK-2 (C) cell lines. All assays were performed in triplicate, and data shown are mean ± SD of three independent experiments. * $p < 0.05$; ** $p < 0.01$; **** $p < 0.0001$. *ns:* no significant. Control = without any treatment; BBR = berberine only; Laser = laser only; BBR + Laser = berberine associated with photodynamic therapy.

Table 1
Differential expression of target genes of anticancer drugs in 786-O cells after treatment with berberine associated with photodynamic therapy.

Gene symbol	Fold regulation	*p*-value
FIGF	−3.23	0.02
TERT	−2.46	0.05
PLK3	2.46	0.001

Table 2
Differential metabolites in 786-O cells after treatment with berberine associated with photodynamic therapy compared with control.

Extracellular metabolites in 786-O cell line	30 minutes after treatment with berberine + laser *p*-value	3 hours after treatment with berberine + laser *p*-value	6 hours after treatment with berberine + laser *p*-value
Cystine	↑ (0.0059)	↑ (0.5794)	↑ (0.3988)
Succinate	- (0.8306)	↑ (0.0164)	↓ (0.6538)
Sarcosine	↑ (0.0079)	↑ (0.0317)	↑ (0.0481)
Formate	↑ (0.1201)	- (0.8413)	↓ (< 0.0001)
Pyridoxine	↑ (0.4952)	↑ (0.8896)	↑ (0.9229)
Niacinamide	↑ (0.0119)	↑ (0.5476)	↓ (0.9650)
Hypoxanthine	↑ (0.0169)	↓ (0.3971)	↑ (0.0015)
Fumarate	↑ (0.0967)	↑ (0.2698)	↑ (0.5526)
Asparagine	↑ (0.1215)	↑ (0.5476)	↑ (0.0490)
Aspartate	↑ (0.1120)	↑ (0.8472)	↑ (0.9001)
Phenylalanine	↑ (0.0375)	↑ (0.2273)	↑ (0.1346)
Glucose	↑ (0.3095)	↑ (0.0317)	↑ (0.0208)
Lysine	↑ (0.4206)	↑ (0.0014)	↑ (0.9606)
Isoleucine	↑ (0.2222)	↑ (0.0159)	↑ (0.1720)
Carnitine	↑ (0.1886)	↓ (0.0307)	↑ (0.3435)
Tyrosine	↑ (0.0819)	↑ (0.0317)	↑ (0.0295)
Leucine	↑ (0.1310)	↑ (0.0952)	↑ (0.0182)
Arginine	↑ (0.2522)	↑ (0.0159)	↑ (0.1802)
Lactate	↑ (0.2233)	↑ (0.1497)	↓ (0.0079)
Alanine	↑ (0.1656)	↑ (0.0588)	↓ (0.0705)
Proline	↑ (0.2190)	↑ (0.0952)	- (0.6015)

increase 3 h after the treatment ($p = 0.0014$). Furthermore, it was also observed that the formate levels decreased significantly 6 h after the treatment (($p < 0.0001$). Similarly, the lactate levels were decrease significantly after 6 h of treatment ($p = 0.0079$) and this metabolite performs very important functions involved in cancer.

4. Discussion

RCC is considered a malignancy with high mortality and despite the great advances in the diagnosis and treatment, the survival remains poor yet. The chemotherapy resistance and metastatic potential are the main causes of poor prognosis of patients [35,36]. Thus, there is an urgent need to develop a novel therapeutic approach for the RCC. In this context, mounting evidence has demonstrated that PDT is significantly effective against several types of cancer [37]. In this study, we evaluate the effect of berberine associated with PDT in ACHN, 786-O, and HK-2 cell lines. Recent studies reported that berberine has characteristics that make it fluorescent [38,39]. Thus, berberine can be used as a photosensitizer agent for PDT, increasing the treatment efficiency and reducing the side effects.

In this study, we observed that berberine showed low cytotoxicity in the dark until 40 μM in tumoral cells. The low cytotoxicity of natural products extract has an advantage over conventional chemotherapeutic that produces strong side effects and decreases the patient quality of life [40]. Fluorescence microscopy images showed an efficient internalization of berberine for all cell lines after 3 h of incubation. Moreover, it was observed presence in cytoplasm and nucleus. A study with glioblastoma and pancreatic carcinoma observed that at 10 μM concentration, berberine is mainly distributed in the cytoplasm and at higher concentrations (50 μM or 150 μM), the signal is clearly visualized both in cytoplasm and nucleus [41].

A good photosensitizer agent for PDT should have excellent photochemical reactivity, low dark toxicity and only be cytotoxic in the presence of light [42,43]. Osteosarcoma, skin carcinoma and lung carcinoma cells treated with only 5 μM of berberine in the absence of light showed 100 % of viability whereas berberine associated with UVA radiation generated 60 % survival after 72 h [44]. In this study, berberine presented high activity against RCC cell lines when associated with PDT. The cellular viability decreases significantly after 24 h of irradiation in all cell lines used in this study, thus we can infer that this treatment is effective against RCC. Although HK-2 has been shown to be more sensitive compared to renal carcinoma cell lines, the damage caused by photodynamic therapy is greatly reduced and limited, directing the light source only to tumor sites [45].

The cellular damage caused by oxidative stress in the intracellular biomolecules, such as protein, lipid, RNA/DNA and reactive species oxygen (ROS) has an important function in the PDT used for cancer treatment; the synergism of photosensitizer agent with a laser causes ROS generation leading to cellular death [46]. Our results demonstrated that there was no ROS production in the berberine alone, but the treatment with berberine and PDT resulted in a significant increase of ROS levels.

In this context, ROS regulate autophagy and apoptosis by interaction with specific signaling molecules [47]. Autophagy is a natural process, where cytoplasmic components are degraded in the lysosome. Although studies have inferred that PDT can induce autophagy, the role

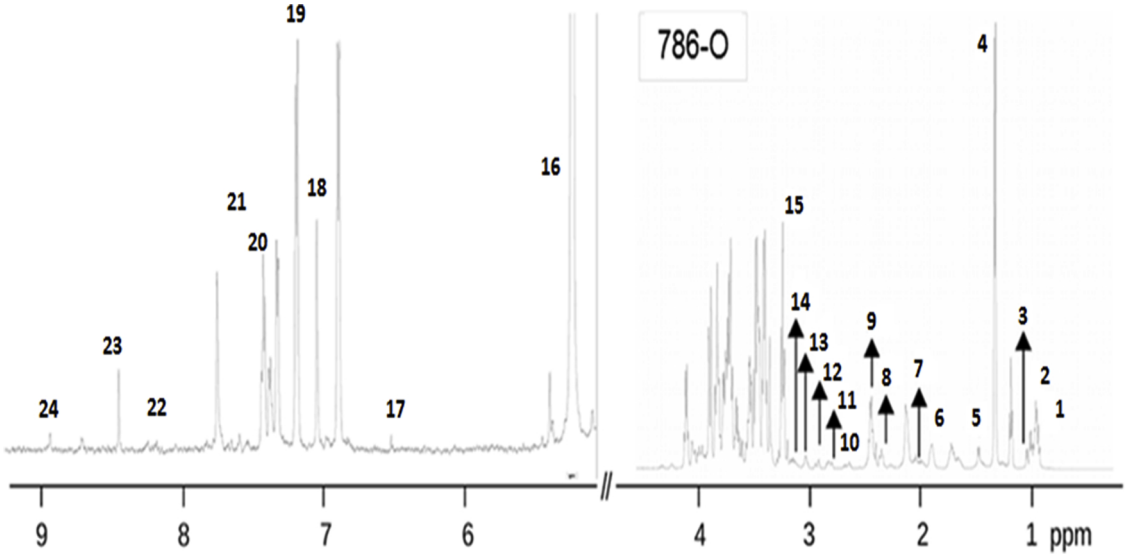

Fig. 7. ^{1}H-NMR spectra from cell lines 786-O 3 h post treatment. Assigned metabolites are: 1 - Isoleucine; 2 - Leucine; 3 - Valine; 4 - Lactate; 5 - Alanine; 6 - Arginine; 7 - Proline; 8 - Succinate; 9 - Glutamine; 10 - Aspartate; 11 - Sarcosine; 12 - Asparagine; 13 - Lysine ; 14 - Cystine; 15 - Carnitine; 16 - Glucose; 17 - Fumarate; 18 - Histidine; 16 - Tyrosine; 20 - Phenylalanine; 21 - Pyridoxine; 22 - Hypoxanthine; 23 - Formate; 24 - Niacinamide.

of autophagy played in PDT is unclear, depending on the context the autophagy process promotes or inhibits cell death by drugs, however, it is quite established that massive ROS production upon treatment can stimulate autophagic cell death [48]. High levels of autophagy may lead to cell death due to expressive degradation of cytoplasm components [49]. In addition, ROS have been demonstrated to activate autophagic death signaling pathway through AMPactivated protein kinase (AMPK)/mechanistic target of rapamycin (mTOR) signaling pathway [50]. Autophagy regulation involves numerous cell signaling and molecular pathways, including microtubule-associated LC3, ATG5/ATG7, mTOR, reactive oxygen species (ROS), and Beclin-1 [51]. In study by Li and cols. (2015) it was observed that the compound silibinin, known to induce oxidative stress in different cell lines, induced autophagy via AMPK/mTOR which was able to inhibit metastatic processes in ACHN and 786-O (renal carcinoma cells), and there was increased expression of the LC3 protein responsible for forming the autophagosomes [52].

It has been previously reported that apoptosis is the major cell death mechanism in the cellular response to PDT, which is associated with characteristic morphological and biochemical modifications [28]. Production of ROS produced induces oxidative stress in mitochondria and pro-apoptotic proteins are released in cytosol activating caspases; when apoptosis is triggered, the nucleases degrade the chromosomal DNA [28,53]. In addition, ROS cause mitochondrial membrane depolarization and/or opening of Bax/Bak channels on the outer mitochondria membrane, which allows release of cytochrome c into the cytosol. Cyt c then forms the apoptosome complex in the cytosol together with Apaf-1 and procaspase-9, leading to caspase-9 activation. Caspase-9 then activates effector caspases such as caspase-3, resulting in cleavage of cellular proteins and cell death by apoptosis [54,55]. For example, dimethoxycurcumin (DMC), one of several synthetic Cur analogues, induced apoptosis in human renal carcinoma cells through the production of ROS, the release of mitochondrial Cyt c, and the subsequent activation of caspase-3 [56].

The activation of caspase-3 is one of the most interesting hallmarks of anticancer of berberine. Berberine induces caspase-3 dependent apoptosis in bladder carcinoma [57], glioblastoma [58], breast carcinoma [59]. Our results showed that an increase of caspase-3 after treatment with berberine and PDT, thus, we can conclude that apoptosis also is modality cell death induced by this treatment. Caspase-3 activation represents the irreversible of execution stage of apoptosis [21].

FIGF gene, also known as *VEGFD*, which presented low expression in 786-O cells after treatment is a member of the vascular endothelial growth factor (*VEGF*) family; these proteins promote angiogenesis and lymphangiogenesis [60]. *VEGF-D* induces growth of the lymphatic vessels via activation of *VEGFR-3* localized on the lymphatic endothelial cells; clinic pathological characteristics have shown that in several human cancers there is a strong correlation between *VEGFR-3* and lymph node metastasis [61]. In addition, *VEGFD* overexpression is correlated with a poor prognosis in ovarian cancer, lung cancer, esophageal squamous cancer and papillary renal carcinoma [61–64].

The human telomerase reverse transcriptase (*TERT*) gene, which also presented low expression in 786-O cells treated with BBR associated with PDT, is essential for the reconstitution of telomerase activity and its expression is highly regulated, being absent or only present in low levels in somatic cells [65]. Up to 90 % of human malignancies have expressive levels of TERT RNA expression, and consequently high TERT enzyme activity [66]. The telomerase activity contributes to their growth advantage and survival of tumor cells [67]. Previous studies demonstrated a strong association with therapy resistance and telomerase expression in breast and gastric cancer patients, in contrast, the low levels of telomerase activity is able to resensitize cell lines to various chemotherapeutics [68].

On the other hand, *PLK3* gene presented high expression in 786-O cells treated with BBR associated with PDT. The polo-like kinases family are important regulators of cellular function and it was associated with cellular responses to DNA damage [69]. *PLK3* gene is downregulated in many human cancers and some studies suggest that it is tumor suppressor [70]. A study observed that *PLK3* null mice are more susceptible to developing tumors in some organs and that low expression is the main mechanism that involves *PLK3* with increased tumorigenesis process [71].

Altogether, disturb in protein expression levels impact a diversity of metabolic pathways. Thus, metabolomics aims to explore the wide range of metabolites that are present in cell lines and biological samples [72]. Currently, it is widely applied in drug discovery, clinical diagnosis, food science and any other fields of human health, moreover, some studies have investigated whether metabolite biomarkers could be used to predict the response to cancer treatment [73,74]. In this study, we observed changes in several metabolites in 786-O cells after treatment with berberine associated with PDT.

The levels of Lysine increased significantly 3 h after the treatment. Lysine is an essential amino acid with several antitumor properties as tumor growth supressor, suggesting it has potential as an anticancer agent [75]. One study evaluated a specific nutrient mixture containing lysine on human renal carcinoma cell line 786-0 and showed significant decrease and complete inhibition of invasion at 1000 μg/ml concentration due to inhibition of matrix metalloproteinases (MMPs). The inhibition of MMP-2 and MMP-9 secretion demonstrated potent antimetastatic action [76]. MMP-2 overexpression detected in cancer tissue is significantly related to larger tumor size and silencing of MMP-9 decreased the migration and invasion in glioma cells [77] once it is known that MMPs can influence the tumor environment by promoting angiogenesis, tumor growth and metastasis [78]. Another study observed that L-arginine and L-lysine solutions affected the splenic sympathetic nerve activity and the proliferation of HCT116 cells (human colon carcinoma) implanted into the subcutaneous space of athymic nude mice [79].

The formate levels decreased significantly after the treatment with BBR and PDT. It is known that the formate is an important molecule whose carbon is incorporated into nucleic acids and into the amino acid serine [80]. A relevant study reported that the formate is a promoter of cancer cell invasion in glioblastoma cells. The cell lines U87, LN229 and NCH601 treated with formate increased cell invasion in a concentration-dependent manner, indicating that formate promotes glioma cell invasion. Subsequently, it was performed knockdown for *MTHFD1L*, the gene encoding for the mitochondrial enzyme responsible for formate production resulting in a significant reduction of invasion relative to control [81].

The levels of lactate also decreased significantly 6 h after the treatment. The relationship between high lactate levels and promotion of cellular malignancy has long been reported [82,83]. The lactate is one of the major metabolites involved and necessary for carcinogenesis, angiogenesis, cell migration and metastasis [82,83]. One of the classical observations of Otto Warburg was the high lactate production rate in malignant cells [84]. A study involving 40 patients with renal cell carcinoma reported high levels of urine lactate before nephrectomy compared to healthy controls. In addition, the levels of lactate and glucose (from which lactate derived) were more abundant in urine samples before nephrectomy than in after ones [85]. The impact of high lactate levels on cell motility is not yet fully elucidated, but there are data showing involvement with signaling protein, such as TGF- β2, that can be a mediator of the lactate-associated effects on migration of cancer cells in glioma cells [83,86]. It is also known that lactate plays an important role in angiogenesis stimulating VEGF protein expression in endothelial cells [87]. Inhibitors of lactate dehydrogenase, enzyme responsible for lactate production, greatly reduced angiogenesis [88].

In summary, we observed that berberine presented low dark cytotoxicity and efficient cellular internalization. The treatment with berberine associated with photodynamic therapy was able to generate ROS and it induces autophagy and apoptosis activating caspase-3. Additionally, three target genes of anti-cancer drugs were differentially

expressed and the treatment with BBR associated with PDT triggered metabolites changes related to inhibition of cell proliferation, migration and angiogenesis.

So, we demonstrated that Berberine is an efficient photosensitizer and its association with photodynamic therapy may be a potential anticancer treatment strategy for renal cancer.

Conflict of interest

The authors declare that they have no competing interests.

Acknowledgments

The authors acknowledge the financial support of the Fundação de Amparo à Pesquisa do Estado de São Paulo (FAPESP) (2009/53989-4) and Coordenação de Aperfeiçoamento de Pessoal de Nível Superior (CAPES) (88882.434430/2019-01).

Appendix A. Supplementary data

Supplementary material related to this article can be found, in the online version, at doi:https://doi.org/10.1016/j.biopha.2019.109794.

References

[1] J.R. Bhatt, A. Finelli, Landmarks in the diagnosis and treatment of renal cell carcinoma, Nature reviews, Urology 11 (9) (2014) 517–525.
[2] S.H. Rossi, T. Klatte, J. Usher-Smith, G.D. Stewart, Epidemiology and screening for renal cancer, World J. Urol. 36 (9) (2018) 1341–1353.
[3] J. Ferlay, I. Soerjomataram, R. Dikshit, S. Eser, C. Mathers, M. Rebelo, D.M. Parkin, D. Forman, F. Bray, Cancer incidence and mortality worldwide: sources, methods and major patterns in GLOBOCAN 2012, Int. J. Cancer 136 (5) (2015) E359–86.
[4] Y. Zhao, H. Tang, X. Zeng, D. Ye, J. Liu, Resveratrol inhibits proliferation, migration and invasion via Akt and ERK1/2 signaling pathways in renal cell carcinoma cells, Biomed. Pharmacother. 98 (2018) 36–44.
[5] Z. Li, P. Hao, Q. Wu, F. Li, J. Zhao, K. Wu, C. Qu, Y. Chen, M. Li, X. Chen, A. Stucky, J. Zhong, L. Li, J.F. Zhong, Genetic mutations associated with metastatic clear cell renal cell carcinoma, Oncotarget 7 (13) (2016) 16172–16179.
[6] D.P. Nguyen, E.A. Vertosick, R.B. Corradi, A. Vilaseca, N.E. Benfante, K.A. Touijer, D.D. Sjoberg, P. Russo, Histological subtype of renal cell carcinoma significantly affects survival in the era of partial nephrectomy, Urol. Oncol. 34 (6) (2016) 259 e1-8.
[7] D. Soulieres, Side-effects associated with targeted therapies in renal cell carcinoma, Curr. Opin. Support. Palliat. Care 7 (3) (2013) 254–257.
[8] E. Rajesh, L.S. Sankari, L. Malathi, J.R. Krupaa, Naturally occurring products in cancer therapy, J. Pharm. Bioallied Sci. 7 (Suppl. 1) (2015) S181–3.
[9] Y. Sun, K. Xun, Y. Wang, X. Chen, A systematic review of the anticancer properties of berberine, a natural product from Chinese herbs, Anti-cancer Drugs 20 (9) (2009) 757–769.
[10] L.M. Ortiz, P. Lombardi, M. Tillhon, A.I. Scovassi, Berberine, an epiphany against cancer, Molecules 19 (8) (2014) 12349–12367.
[11] P. Jabbarzadeh Kaboli, A. Rahmat, P. Ismail, K.H. Ling, Targets and mechanisms of berberine, a natural drug with potential to treat cancer with special focus on breast cancer, Eur. J. Pharmacol. 740 (2014) 584–595.
[12] Z.H. Huang, H.F. Zheng, W.L. Wang, Y. Wang, L.F. Zhong, J.L. Wu, Q.X. Li, Berberine targets epidermal growth factor receptor signaling to suppress prostate cancer proliferation in vitro, Mol. Med. Rep. 11 (3) (2015) 2125–2128.
[13] E. Barzegar, S. Fouladdel, T.K. Movahhed, S. Atashpour, M.H. Ghahremani, S.N. Ostad, E. Azizi, Effects of berberine on proliferation, cell cycle distribution and apoptosis of human breast cancer T47D and MCF7 cell lines, Iran. J. Basic Med. Sci. 18 (4) (2015) 334–342.
[14] C.M. Tsang, K.C. Cheung, Y.C. Cheung, K. Man, V.W. Lui, S.W. Tsao, Y. Feng, Berberine suppresses Id-1 expression and inhibits the growth and development of lung metastases in hepatocellular carcinoma, Biochim. Biophys. Acta 1852 (3) (2015) 541–551.
[15] S.H. Park, J.H. Sung, E.J. Kim, N. Chung, Berberine induces apoptosis via ROS generation in PANC-1 and MIA-PaCa2 pancreatic cell lines, Braz. J. Med. Biol. Res. 48 (2) (2015) 111–119.
[16] J. Li, L. Gu, H. Zhang, T. Liu, D. Tian, M. Zhou, S. Zhou, Berberine represses DAXX gene transcription and induces cancer cell apoptosis, Lab. Invest. J. Tech. Methods Pathol. 93 (3) (2013) 354–364.
[17] B.J. Philogene, J.T. Arnason, G.H. Towers, Z. Abramowski, F. Campos, D. Champagne, D. McLachlan, Berberine: a naturally occurring phototoxic alkaloid, J. Chem. Ecol. 10 (1) (1984) 115–123.
[18] L.L. Cheng, M. Wang, H. Zhu, K. Li, R.R. Zhu, X.Y. Sun, S.D. Yao, Q.S. Wu, S.L. Wang, Characterization of the transient species generated by the photoionization of Berberine: a laser flash photolysis study, Spectrochim. Acta A. Mol. Biomol. Spectrosc. 73 (5) (2009) 955–959.
[19] S. Jantova, S. Letasiova, V. Brezova, L. Cipak, J. Labaj, Photochemical and phototoxic activity of berberine on murine fibroblast NIH-3T3 and Ehrlich ascites carcinoma cells, J. Photochem. Photobiol. B, Biol. 85 (3) (2006) 163–176.
[20] J.J. Inbaraj, B.M. Kukielczak, P. Bilski, S.L. Sandvik, C.F. Chignell, Photochemistry and photocytotoxicity of alkaloids from Goldenseal (Hydrastis canadensis L.) 1. Berberine, Chem. Res. Toxicol. 14 (11) (2001) 1529–1534.
[21] A. Castilho-Fernandes, T.G. Lopes, F.L. Primo, M.R. Pinto, A.C. Tedesco, Photodynamic process induced by chloro-aluminum phthalocyanine nanoemulsion in glioblastoma, Photodiagnosis Photodyn. Ther. 19 (2017) 221–228.
[22] T. Osaki, I. Yokoe, K. Takahashi, K. Inoue, M. Ishizuka, T. Tanaka, K. Azuma, Y. Murahata, T. Tsuka, N. Itoh, T. Imagawa, Y. Okamoto, Metformin enhances the cytotoxicity of 5-aminolevulinic acid-mediated photodynamic therapy in vitro, Oncol. Lett. 14 (1) (2017) 1049–1053.
[23] P. Agostinis, K. Berg, K.A. Cengel, T.H. Foster, A.W. Girotti, S.O. Gollnick, S.M. Hahn, M.R. Hamblin, A. Juzeniene, D. Kessel, M. Korbelik, J. Moan, P. Mroz, D. Nowis, J. Piette, B.C. Wilson, J. Golab, Photodynamic therapy of cancer: an update, CA Cancer J. Clin. 61 (4) (2011) 250–281.
[24] W. Kuzyniak, J. Schmidt, W. Glac, J. Berkholz, G. Steinemann, B. Hoffmann, E.A. Ermilov, A.G. Gurek, V. Ahsen, B. Nitzsche, M. Hopfner, Novel zinc phthalocyanine as a promising photosensitizer for photodynamic treatment of esophageal cancer, Int. J. Oncol. 50 (3) (2017) 953–963.
[25] D. Kessel, N.L. Oleinick, Cell death pathways associated with photodynamic therapy: an update, Photochem. Photobiol. 94 (2) (2018) 213–218.
[26] B.S. Erikstein, H.R. Hagland, J. Nikolaisen, M. Kulawiec, K.K. Singh, B.T. Gjertsen, K.J. Tronstad, Cellular stress induced by resazurin leads to autophagy and cell death via production of reactive oxygen species and mitochondrial impairment, J. Cell. Biochem. 111 (3) (2010) 574–584.
[27] P. Tu, Q. Huang, Y. Ou, X. Du, K. Li, Y. Tao, H. Yin, Aloe-emodin-mediated photodynamic therapy induces autophagy and apoptosis in human osteosarcoma cell line MG63 through the ROS/JNK signaling pathway, Oncol. Rep. 35 (6) (2016) 3209–3215.
[28] T.J. Dougherty, C.J. Gomer, B.W. Henderson, G. Jori, D. Kessel, M. Korbelik, J. Moan, Q. Peng, Photodynamic therapy, J. Natl. Cancer Inst. 90 (12) (1998) 889–905.
[29] A. Oniszczuk, K.A. Wojtunik-Kulesza, T. Oniszczuk, K. Kasprzak, The potential of photodynamic therapy (PDT)-Experimental investigations and clinical use, Biomed. Pharmacother. 83 (2016) 912–929.
[30] M.S. Diaz, M.L. Freile, M.I. Gutierrez, Solvent effect on the UV/Vis absorption and fluorescence spectroscopic properties of berberine, Photochem. Photobiol. Sci. 8 (7) (2009) 970–974.
[31] D.B. Kell, M. Brown, H.M. Davey, W.B. Dunn, I. Spasic, S.G. Oliver, Metabolic footprinting and systems biology: the medium is the message, Nature reviews, Microbiology 3 (7) (2005) 557–565.
[32] G.A. Pope, D.A. MacKenzie, M. Defernez, M.A. Aroso, L.J. Fuller, F.A. Mellon, W.B. Dunn, M. Brown, R. Goodacre, D.B. Kell, M.E. Marvin, E.J. Louis, I.N. Roberts, Metabolic footprinting as a tool for discriminating between brewing yeasts, Yeast 24 (8) (2007) 667–679.
[33] D.S. Wishart, T. Jewison, A.C. Guo, M. Wilson, C. Knox, Y. Liu, Y. Djoumbou, R. Mandal, F. Aziat, E. Dong, S. Bouatra, I. Sinelnikov, D. Arndt, J. Xia, P. Liu, F. Yallou, T. Bjorndahl, R. Perez-Pineiro, R. Eisner, F. Allen, V. Neveu, R. Greiner, A. Scalbert, HMDB 3.0–the human metabolome database in 2013, Nucleic Acids Res. 41 (Database issue) (2013) D801–7.
[34] J. Chong, O. Soufan, C. Li, I. Caraus, S. Li, G. Bourque, D.S. Wishart, J. Xia, MetaboAnalyst 4.0: towards more transparent and integrative metabolomics analysis, Nucleic Acids Res. 46 (W1) (2018) W486–W494.
[35] Q. Zhang, J. Shi, F. Yuan, H. Wang, W. Fu, J. Pan, Y. Huang, J. Yu, J. Yang, Z. Chen, Higher expression of XPF is a critical factor in intrinsic chemotherapy resistance of human renal cell carcinoma, Int. J. Cancer 139 (12) (2016) 2827–2837.
[36] C. Yang, Y. Li, L. Fu, T. Jiang, F. Meng, Betulinic acid induces apoptosis and inhibits metastasis of human renal carcinoma cells in vitro and in vivo, J. Cell. Biochem. (2018).
[37] Z. Zhou, J. Song, L. Nie, X. Chen, Reactive oxygen species generating systems meeting challenges of photodynamic cancer therapy, Chem. Soc. Rev. 45 (23) (2016) 6597–6626.
[38] L. Xu, S. Hong, N. Sun, K. Wang, L. Zhou, L. Ji, R. Pei, Berberine as a novel light-up i-motif fluorescence ligand and its application in designing molecular logic systems, Chem. Commun. 52 (1) (2016) 179–182.
[39] C.Q. Zhou, J.W. Yang, C. Dong, Y.M. Wang, B. Sun, J.X. Chen, Y.S. Xu, W.H. Chen, Highly selective, sensitive and fluorescent sensing of dimeric G-quadruplexes by a dimeric berberine, Org. Biomol. Chem. 14 (1) (2016) 191–197.
[40] M. Li, M. Zhang, Z.L. Zhang, N. Liu, X.Y. Han, Q.C. Liu, W.J. Deng, C.X. Liao, Induction of apoptosis by berberine in hepatocellular carcinoma HepG2 cells via downregulation of NF-kappaB, Oncol. Res. 25 (2) (2017) 233–239.
[41] A. Agnarelli, M. Natali, M. Garcia-Gil, R. Pesi, M.G. Tozzi, C. Ippolito, N. Bernardini, R. Vignali, R. Batistoni, A.M. Bianucci, S. Marracci, Cell-specific pattern of berberine pleiotropic effects on different human cell lines, Sci. Rep. 8 (1) (2018) 10599.
[42] H. Abrahamse, M.R. Hamblin, New photosensitizers for photodynamic therapy, Biochem. J. 473 (4) (2016) 347–364.
[43] J. Zhang, C. Jiang, J.P. Figueiro Longo, R.B. Azevedo, H. Zhang, L.A. Muehlmann, An updated overview on the development of new photosensitizers for anticancer photodynamic therapy, Acta Pharm. Sin. B 8 (2) (2018) 137–146.
[44] R. Bhattacharyya, B. Saha, M. Tyagi, S.K. Bandyopadhyay, B.S. Patro, S. Chattopadhyay, Differential modes of photosensitisation in cancer cells by berberine and coralyne, Free Radic. Res. 51 (7–8) (2017) 723–738.
[45] B. Karakullukcu, K. van Oudenaarde, M.P. Copper, W.M. Klop, R. van Veen,

M. Wildeman, I. Bing Tan, Photodynamic therapy of early stage oral cavity and oropharynx neoplasms: an outcome analysis of 170 patients, Eur. Arch. Otorhinolaryngol. 268 (2) (2011) 281–288.
[46] P.H. Tu, W.J. Huang, Z.L. Wu, Q.Z. Peng, Z.B. Xie, J. Bao, M.H. Zhong, Induction of cell death by pyropheophorbide-alpha methyl ester-mediated photodynamic therapy in lung cancer A549 cells, Cancer Med. 6 (3) (2017) 631–639.
[47] Z. Zou, H. Chang, H. Li, S. Wang, Induction of reactive oxygen species: an emerging approach for cancer therapy, Apoptosis 22 (11) (2017) 1321–1335.
[48] L. Poillet-Perez, G. Despouy, R. Delage-Mourroux, M. Boyer-Guittaut, Interplay between ROS and autophagy in cancer cells, from tumor initiation to cancer therapy, Redox Biol. 4 (2015) 184–192.
[49] V. Inguscio, E. Panzarini, L. Dini, Autophagy contributes to the death/survival balance in cancer photo dynamic therapy, Cells 1 (3) (2012) 464–491.
[50] J. Sun, Y. Feng, Y. Wang, Q. Ji, G. Cai, L. Shi, Y. Wang, Y. Huang, J. Zhang, Q. Li, Alpha-hederin induces autophagic cell death in colorectal cancer cells through reactive oxygen species dependent AMPK/mTOR signaling pathway activation, Int. J. Oncol. 54 (5) (2019) 1601–1612.
[51] H.L. Yang, R.W. Lin, P. Karuppaiya, D.C. Mathew, T.D. Way, H.C. Lin, C.C. Lee, Y.C. Hseu, Induction of autophagic cell death in human ovarian carcinoma cells by Antrodia salmonea through increased reactive oxygen species generation, J. Cell. Physiol. 234 (7) (2019) 10747–10760.
[52] F. Li, Z. Ma, Z. Guan, Y. Chen, K. Wu, P. Guo, X. Wang, D. He, J. Zeng, Autophagy induction by silibinin positively contributes to its anti-metastatic capacity via AMPK/mTOR pathway in renal cell carcinoma, Int. J. Mol. Sci. 16 (4) (2015) 8415–8429.
[53] W. Li, Q. Xie, L. Lai, Z. Mo, X. Peng, E. Leng, D. Zhang, H. Sun, Y. Li, W. Mei, S. Gao, In vitro evaluation of ruthenium complexes for photodynamic therapy, Photodiagnosis Photodyn. Ther. 18 (2017) 83–94.
[54] P. Pallepati, D. Averill-Bates, Mild thermotolerance induced at 40 degrees C increases antioxidants and protects HeLa cells against mitochondrial apoptosis induced by hydrogen peroxide: role of p53, Arch. Biochem. Biophys. 495 (2) (2010) 97–111.
[55] S. Orrenius, V. Gogvadze, B. Zhivotovsky, Calcium and mitochondria in the regulation of cell death, Biochem. Biophys. Res. Commun. 460 (1) (2015) 72–81.
[56] J.W. Lee, H.M. Hong, D.D. Kwon, H.O. Pae, H.J. Jeong, Dimethoxycurcumin, a structural analogue of curcumin, induces apoptosis in human renal carcinoma caki cells through the production of reactive oxygen species, the release of cytochrome C, and the activation of caspase-3, Korean J. Urol. 51 (12) (2010) 870–878.
[57] K. Yan, C. Zhang, J. Feng, L. Hou, L. Yan, Z. Zhou, Z. Liu, C. Liu, Y. Fan, B. Zheng, Z. Xu, Induction of G1 cell cycle arrest and apoptosis by berberine in bladder cancer cells, Eur. J. Pharmacol. 661 (1–3) (2011) 1–7.
[58] J. Wang, Q. Qi, Z. Feng, X. Zhang, B. Huang, A. Chen, L. Prestegarden, X. Li, J. Wang, Berberine induces autophagy in glioblastoma by targeting the AMPK/mTOR/ULK1-pathway, Oncotarget 7 (41) (2016) 66944–66958.
[59] Y. Pan, F. Zhang, Y. Zhao, D. Shao, X. Zheng, Y. Chen, K. He, J. Li, L. Chen, Berberine enhances chemosensitivity and induces apoptosis through dose-orchestrated AMPK signaling in breast cancer, J. Cancer 8 (9) (2017) 1679–1689.
[60] S.A. Stacker, M.G. Achen, Emerging roles for VEGF-D in human disease, Biomolecules 8 (1) (2018).
[61] S. Bierer, E. Herrmann, T. Kopke, J. Neumann, E. Eltze, L. Hertle, C. Wulfing, Lymphangiogenesis in kidney cancer: expression of VEGF-C, VEGF-D and VEGFR-3 in clear cell and papillary renal cell carcinoma, Oncol. Rep. 20 (4) (2008) 721–725.
[62] X. Qi, L. Du, X. Chen, L. Chen, T. Yi, X. Chen, Y. Wen, Y. Wei, X. Zhao, VEGF-D-enhanced lymph node metastasis of ovarian cancer is reversed by vesicular stomatitis virus matrix protein, Int. J. Oncol. 49 (1) (2016) 123–132.
[63] J. Ming, Q. Zhang, X. Qiu, E. Wang, Interleukin 7/interleukin 7 receptor induce c-Fos/c-Jun-dependent vascular endothelial growth factor-D up-regulation: a mechanism of lymphangiogenesis in lung cancer, Eur. J. Cancer 45 (5) (2009) 866–873.
[64] Z. Yang, Y.G. Wang, K. Su, VEGF-C and VEGF-D expression and its correlation with lymph node metastasis in esophageal squamous cell cancer tissue, Asian Pac. J. Cancer Prev.: APJCP 16 (1) (2015) 271–274.
[65] A. Pestana, J. Vinagre, M. Sobrinho-Simoes, P. Soares, TERT biology and function in cancer: beyond immortalisation, J. Mol. Endocrinol. 58 (2) (2017) R129–R146.
[66] J. Casuscelli, M.F. Becerra, B.J. Manley, E.C. Zabor, E. Reznik, A. Redzematovic, M.E. Arcila, D.M. Tennenbaum, M. Ghanaat, M. Kashan, C.G. Stief, M. Carlo, M.H. Voss, D.R. Feldman, R.J. Motzer, Y. Chen, V.E. Reuter, J.A. Coleman, P. Russo, J.J. Hsieh, A.A. Hakimi, Characterization and impact of TERT promoter region mutations on clinical outcome in renal cell carcinoma, Eur. Urol. Focus (2017).
[67] M. Gay-Bellile, L. Veronese, P. Combes, E. Eymard-Pierre, F. Kwiatkowski, M.M. Dauplat, A. Cayre, M. Privat, C. Abrial, Y.J. Bignon, M.A. Mouret-Reynier, P. Vago, F. Penault-Llorca, A. Tchirkov, TERT promoter status and gene copy number gains: effect on TERT expression and association with prognosis in breast cancer, Oncotarget 8 (44) (2017) 77540–77551.
[68] Y. Xu, A. Goldkorn, Telomere and telomerase therapeutics in cancer, Genes 7 (6) (2016).
[69] M. Bahassi el, C.W. Conn, D.L. Myer, R.F. Hennigan, C.H. McGowan, Y. Sanchez, P.J. Stambrook, Mammalian Polo-like kinase 3 (Plk3) is a multifunctional protein involved in stress response pathways, Oncogene 21 (43) (2002) 6633–6640.
[70] C. Helmke, M. Raab, F. Rodel, Y. Matthess, T. Oellerich, R. Mandal, M. Sanhaji, H. Urlaub, C. Rodel, S. Becker, K. Strebhardt, Ligand stimulation of CD95 induces activation of Plk3 followed by phosphorylation of caspase-8, Cell Res. 26 (8) (2016) 914–934.
[71] D. Xu, W. Dai, C. Li, Polo-like kinase 3, hypoxic responses, and tumorigenesis, Cell Cycle 16 (21) (2017) 2032–2036.
[72] Y. Nan, X. Zhou, Q. Liu, A. Zhang, Y. Guan, S. Lin, L. Kong, Y. Han, X. Wang, Serum metabolomics strategy for understanding pharmacological effects of ShenQi pill acting on kidney yang deficiency syndrome, J. Chromatogr. B Analyt. Technol. Biomed. Life Sci. 1026 (2016) 217–226.
[73] A. Zhang, H. Sun, G. Yan, P. Wang, X. Wang, Metabolomics for biomarker discovery: moving to the clinic, BioMed Res. Int. 2015 (2015) 354671.
[74] T. Iemoto, S. Nishiumi, T. Kobayashi, S. Fujigaki, T. Hamaguchi, K. Kato, H. Shoji, Y. Matsumura, K. Honda, M. Yoshida, Serum level of octanoic acid predicts the efficacy of chemotherapy for colorectal cancer, Oncol. Lett. 17 (1) (2019) 831–842.
[75] M.W. Roomi, V. Ivanov, T. Kalinovsky, A. Niedzwiecki, M. Rath, Effect of ascorbic acid, lysine, proline, and green tea extract on human osteosarcoma cell line MNNG-HOS xenografts in nude mice: evaluation of tumor growth and immunohistochemistry, Med. Oncol. 23 (3) (2006) 411–417.
[76] M.W. Roomi, V. Ivanov, T. Kalinovsky, A. Niedzwiecki, M. Rath, Anticancer effect of lysine, proline, arginine, ascorbic acid and green tea extract on human renal adenocarcinoma line 786-0, Oncol. Rep. 16 (5) (2006) 943–947.
[77] J. Cathcart, A. Pulkoski-Gross, J. Cao, Targeting matrix metalloproteinases in cancer: bringing new life to old ideas, Genes Dis. 2 (1) (2015) 26–34.
[78] A.H. Webb, B.T. Gao, Z.K. Goldsmith, A.S. Irvine, N. Saleh, R.P. Lee, J.B. Lendermon, R. Bheemreddy, Q. Zhang, R.C. Brennan, D. Johnson, J.J. Steinle, M.W. Wilson, V.M. Morales-Tirado, Inhibition of MMP-2 and MMP-9 decreases cellular migration, and angiogenesis in in vitro models of retinoblastoma, BMC Cancer 17 (1) (2017) 434.
[79] J. Shen, Y. Horii, Y. Fujisaki, K. Nagai, Effects of L-arginine and L-lysine mixtures on splenic sympathetic nerve activity and tumor proliferation, Auton. Neurosci.: Basic Clin. 147 (1–2) (2009) 86–90.
[80] S.G. Lamarre, G. Morrow, L. Macmillan, M.E. Brosnan, J.T. Brosnan, Formate: an essential metabolite, a biomarker, or more? Clin. Chem. Lab. Med. 51 (3) (2013) 571–578.
[81] J. Meiser, A. Schuster, M. Pietzke, J. Vande Voorde, D. Athineos, K. Oizel, G. Burgos-Barragan, N. Wit, S. Dhayade, J.P. Morton, E. Dornier, D. Sumpton, G.M. Mackay, K. Blyth, K.J. Patel, S.P. Niclou, A. Vazquez, Increased formate overflow is a hallmark of oxidative cancer, Nat. Commun. 9 (1) (2018) 1368.
[82] M.L. Goodwin, Z. Pennington, E.M. Westbroek, E. Cottrill, A.K. Ahmed, D.M. Sciubba, Lactate and cancer: a "lactatic" perspective on spinal tumor metabolism (part 1), Ann. Transl. Med. 7 (10) (2019) 220.
[83] F. Hirschhaeuser, U.G. Sattler, W. Mueller-Klieser, Lactate: a metabolic key player in cancer, Cancer Res. 71 (22) (2011) 6921–6925.
[84] I. San-Millan, G.A. Brooks, Reexamining cancer metabolism: lactate production for carcinogenesis could be the purpose and explanation of the Warburg Effect, Carcinogenesis 38 (2) (2017) 119–133.
[85] R. Ragone, F. Sallustio, S. Piccinonna, M. Rutigliano, G. Vanessa, S. Palazzo, G. Lucarelli, P. Ditonno, M. Battaglia, F.P. Fanizzi, F.P. Schena, Renal cell carcinoma: a study through NMR-based metabolomics combined with transcriptomics, Diseases 4 (1) (2016).
[86] F. Baumann, P. Leukel, A. Doerfelt, C.P. Beier, K. Dettmer, P.J. Oefner, M. Kastenberger, M. Kreutz, T. Nickl-Jockschat, U. Bogdahn, A.K. Bosserhoff, P. Hau, Lactate promotes glioma migration by TGF-beta2-dependent regulation of matrix metalloproteinase-2, Neuro-oncology 11 (4) (2009) 368–380.
[87] F. Polet, O. Feron, Endothelial cell metabolism and tumour angiogenesis: glucose and glutamine as essential fuels and lactate as the driving force, J. Intern. Med. 273 (2) (2013) 156–165.
[88] T.K. Hunt, R. Aslam, Z. Hussain, S. Beckert, Lactate, with oxygen, incites angiogenesis, Adv. Exp. Med. Biol. 614 (2008) 73–80.

Biomedicine & Pharmacotherapy 136 (2021) 111175

Contents lists available at ScienceDirect

Biomedicine & Pharmacotherapy

journal homepage: www.elsevier.com/locate/biopha

Corrigendum to "Berberine associated photodynamic therapy promotes autophagy and apoptosis via ROS generation in renal carcinoma cells" [Biomed. Pharmacother. 123 (2020) 109794]

Tairine Zara Lopes [a], Fabio Rogério de Moraes [b,c], Antonio Claudio Tedesco [d], Raghuvir Krishnaswamy Arni [b,c], Paula Rahal [a], Marilia Freitas Calmon [a,*]

[a] Laboratory of Genomics Studies, São Paulo State University, São José do Rio Preto, São Paulo, Brazil
[b] Physics Department, São Paulo State University, São José do Rio Preto, São Paulo, Brazil
[c] Multiuser Center for Biomolecular Innovation, São Paulo State University, São José do Rio Preto, São Paulo, Brazil
[d] Department of Chemistry, Center of Nanotechnology and Tissue Engineering-Photobiology and Photomedicine Research Group, Faculty of Philosophy, Sciences and Letters of Ribeirao Preto, University of São Paulo, Ribeirao Preto, SP, Brazil

The authors regret the lack of the National Council for Scientific and Technological Development – CNPq grant number 307064/2018-2 in the Acknowledgments section of the original article. The authors would like to apologise for any inconvenience caused.

DOI of original article: https://doi.org/10.1016/j.biopha.2019.109794.
* Corresponding author.
E-mail address: marilia.calmon@unesp.br (M.F. Calmon).

https://doi.org/10.1016/j.biopha.2020.111175

Available online 24 December 2020

Biomedicine & Pharmacotherapy 125 (2020) 110038

Contents lists available at ScienceDirect

Biomedicine & Pharmacotherapy

journal homepage: www.elsevier.com/locate/biopha

Corrigendum

Corrigendum to "Berberine associated photodynamic therapy promotes autophagy and apoptosis via ROS generation in renal carcinoma cells" [Biomed. Pharmacother., v.123 (2020) 109794]

Tairine Zara Lopes[a], Fabio Rogério de Moraes[b,c], Antonio Claudio Tedesco[d], Raghuvir Krishnaswamy Arni[b,c], Paula Rahal[a], Marilia Freitas Calmon[a,*]

[a] Laboratory of Genomics Studies, São Paulo State University, São José do Rio Preto, São Paulo, Brazil
[b] Physics Department, São Paulo State University, São José do Rio Preto, São Paulo, Brazil
[c] Multiuser Center for Biomolecular Innovation, São Paulo State University, São José do Rio Preto, São Paulo, Brazil
[d] Department of Chemistry, Center of Nanotechnology and Tissue Engineering-Photobiology and Photomedicine Research Group, Faculty of Philosophy, Sciences and Letters of Ribeirao Preto, University of São Paulo, Ribeirao Preto, SP, Brazil

The authors regret the lack of the grant numbers FAPESP 2015/13765-0; FAPESP 2015/16660-5; FAPESP 2014/22198-0 in the Acknowledgments section of the original article.

The authors would like to apologise for any inconvenience caused.

DOI of original article: https://doi.org/10.1016/j.biopha.2019.109794

* Corresponding author at: Department of Biology, Instituto de Biociências, Letras e Ciências Exatas – IBILCE/UNESP, Cristóvão Colombo, 2265, 15054-000, São José do Rio Preto, SP, Brazil.
E-mail address: marilia.calmon@unesp.br (M.F. Calmon).

https://doi.org/10.1016/j.biopha.2020.110038